Modification of Activated Carbon from *Elaeis Guineensis Jacq Shell* with Magnetite (Fe_3O_4) Particles and Study Adsorption-Desorption on Ni(II) Ions in Solution

Modification of Activated Carbon from *Elaeis Guineensis Jacq Shell* with Magnetite (Fe_3O_4) Particles and Study Adsorption-Desorption on Ni(II) Ions in Solution

A S Zulaicha[1,2*], **Buhani**[3*], **Suharso**[3]

[1] Sumatera Institute of Technology, Faculty of Sciences, Jl. Terusan Ryacudu, Way Huwi, Jati Agung, South Lampung, Indonesia
[2] Graduate School of Chemistry, University of Lampung, Jl. Sumantri Brojonegoro No 1, Bandar Lampung, Indonesia
[3] Department of Chemistry, Faculty of Mathematics and Natural Sciences, University of Lampung, Jl. Sumantri Brojonegoro no 1, Bandar Lampung, Indonesia

email: annisaa.zulaicha@km.itera.ac.id[1,2], buhani@fmipa.unila.ac.id[1]

Abstract. Activated carbon coated with magnetite (ACA-Fe_3O_4) was synthesized in this study. Activated carbon was synthesized using an *Elaeis Guineensis Jacq* (EGJ) as a raw material followed by physical and chemical activation. Physical activation is carried out by heating at a temperature of 700°C and followed by a reaction with H_3PO_4 solution as chemical activation. Furthermore, the activated carbon was reacted with a mixture of $FeCl_3$ and $FeSO_4$ solution then followed by the addition of NaOH solution up to a pH of 10. Characterization with X-Ray Diffraction (XRD) and Scanning Electron Microscopy - Energy Dispersive X-Ray (SEM-EDX) on ACA-Fe_3O_4 was done to confirm that magnetite has succeeded to coating on ACA. Brunauer-Emmett-Teller Surface Area Method (S_{BET}) confirmed that pore volume and average pore diameter increase with the presence of magnetite. Optimum conditions for Ni(II) ion adsorption with ACA- Fe_3O_4 was under conditions of 0.5 grams adsorbent, 25 mL of Ni(II) ion solution 100 ppm, and contact time of 1 hour with the acquisition of 99.11%. Adsorption process more suitable with pseudo-second-order and Langmuir adsorption isotherm pattern. Desorption of Ni(II) ion of 70.84% using HCl.

Keyword: *Elaeis Guineensis Jacq*, Magnetite activated carbon, Adsorption, Desorption, Ni(II)

1. Introduction

Increased industrial development is a consequence of an environmental crisis [1]. At present, one of the environmental crises is pollution in waters with industrial wastes such as heavy metals [2, 3]. Known heavy metals such as Pb, Cd, Cu, Ni, and Zn that accumulate in waters reach more than 7×10^5 tons and cannot be degraded in the environment [4,5].

Heavy metals that accumulate in waters can enter the food chain and cause harm to humans [6,7]. The most amount of nickel metal is 3% of the earth's composition [8]. Besides, the World Health

Organization (WHO) and the United States Environmental Protection Agency (USEPA) states the maximum permissible limit of Ni (II) ions in drinking water is 0.02 $mg \cdot L^{-1}$ [9,10].

Several methods have been developed to reduce waste in the form of heavy metals, such as chemical precipitation, coagulation, extraction, and adsorption [12]. According to Wang and Li [13], some of these conventional methods are less efficient because of complicated and expensive and they can produce other products that are poisonous. Among the methods, adsorption is a very effective separation technique because the method is simple, inexpensive, and environmentally friendly [15].

Palm oil is the mainstay commodity of the State of Indonesia. 60% of the oil palm shell waste is directly produced from oil production. Oil palm shells containing 45% cellulose and 26% hemicellulose can be processed into products that have high economic value, namely as activated carbon [14]. Activated carbon (powder) is the most efficient adsorbent used to remove heavy metals [17, 21-23].

The adsorption capacity of the active side (pore) of activated carbon is very large so that it is widely used as an adsorbent for heavy metal waste in waters [24]. However, activated carbon has a light molecular weight making it difficult to separate adsorbent from adsorbate in the form of solution. The lack of activated carbon inhibits the process of separating metal ions from solution. For this reason, it is necessary to further modify activated carbon in increasing its use as a heavy metal adsorbent [18]. Coating of activated carbon using magnetite particles (Fe_3O_4) can produce the adsorbent which has a large capacity, selectivity towards target metal ions, and quick separation process because of the magnetic properties of adsorbent [19-20, 25].

Furthermore, desorption on adsorbents that have bind heavy metal ions is carried out [16, 26]. The process of adsorption-desorption of Ni(II) ions in a solution using activated carbon magnetite from a coconut shell has been studied in this study. The adsorption data obtained were evaluated using the Langmuir and Freundlich adsorption isotherm models and the adsorption kinetics refer to pseudo-first-order and pseudo-second-order [27]. Desorption data strengthen and confirm metal ions that have been absorbed and are also used as consideration for repeated use of adsorbents.

2. **Experimental·**

2.1. Material and Instrumentation

Raw materials in the synthesis of ACA-Fe_3O_4 were a clean and dry EGJ shell. Other materials were filter paper, aluminum foil, universal pH indicator, $Ni(NO_3)_2 \cdot 6H_2O$, $FeSO_4 \cdot 7H_2O$, $FeCl_3$, NaOH, H_3PO_4, and aquades. Glass equipment was used in this study. In addition to glassware, analytical balance, crusher, siever, Heraeus KR170E0 type furnace, magnetic stirrer, shaker, centrifuge, and pH meter were also used. XRD, SEM-EDX (JEOL-JSN-6510LA), BET Surface Area (NOVA touch 4LX), and AAS (PERKIN ELMER model 3110) were the instruments used in this study.

2.2. Preparation of Activated Carbon

Carbon was obtained from carbonized oil palm shells in the conductor's vessels. The carbon produced was inserted into the sieve with a size of 100-200 µm. The carbon powder was placed in the furnace at a temperature of 700°C for 1 hour to open the carbon pores so that it is activated physically (AC). Furthermore, carbon activation was carried out chemically by soaking using a 10% H_3PO_4 solution for 24 hours according to the procedures [14] to produce activated carbon physics-chemistry (ACA).

2.3. Activated Carbon Coating

Magnetite coating on activated carbon was prepared according to method given by Mohan et al. [28]. The Fe^{3+}/Fe^{2+} solution was used to modify activated carbon into activated carbon magnetite (Fe_3O_4). The Fe^{3+}/Fe^{2+} solution was obtained from a mixture of $FeCl_3$ and $FeSO_4$ solution at 60°C in 30 minutes. The composition of the $FeCl_3$ solution 1.33 gram $FeCl_3$ in 130 mL aquades. Then the $FeSO_4$ solution

was made from 6 grams of $FeSO_4 \cdot 7H_2O$ in 15 mL of distilled water. At 60°C for 30 minutes the both solutions were stirred. Furthermore, the suspension was added ACA-Fe_3O_4 and stirred again for 30 minutes. The suspension of ACA-Fe_3O_4 was obtained by mixing 5 grams of ACA into 50 ml of distilled water. The mixture was adjusted to pH 10 using a 10 M NaOH solution. Then it was rinsed to neutral pH with distilled water and dried in an oven at 50°C for 5 hours.

2.4. Adsorbent Characterization

Identification of the crystalline phase from ACA and ACA-Fe_3O_4 used X-ray diffraction (XRD) (PANalytical model X'Pert PRO) with Cu-Kα radiation (λ = 1.54Å) and scanned from 5° to 60°. Morphology and elemental composition of ACA and ACA-Fe_3O_4 was determined by SEM-EDX characterization. Data of surface area, pore volume, and adsorption-desorption patterns of ACA and ACA-Fe_3O_4 were obtained from the results of BET surface area.

2.5. Adsorption-Desorption Test

Test of adsorption of Ni(II) ions on ACA-Fe_3O_4 included determination of optimum dose of adsorbent, the influence of pH, contact time, and adsorbate concentration on ACA and ACA-Fe_3O_4 using the Batch Method. Variation of the adsorbent dose by entering 100-500 mg of adsorbent into 25 ml of 100 ppm Ni(II) solution then stirring using a magnetic stirrer for 1 hour. The resulted mixture was deposited, decanted, and centrifuged hence the concentration of the filtrate was known from AAS. The optimum dose obtained was used for the determination of pH carried out at pH 3, 4, 5, 6, 7, 8, 9, and 10. Contact time with variations of 0, 15, 30, 60, and 90 minutes was carried out with the same procedure in the optimum dosage of adsorbent and pH. The concentrations were made variations of 0, 25, 50, 100, 150, 200, and 250 ppm using optimum conditions to determine the effect of concentration on the adsorption of Ni(II) ions both in ACA and ACA-Fe_3O_4. Then the desorption process was carried out using distilled water, ethanol, HCl solution, and EDTA in the adsorbent which had been used in the adsorption process, stirred for 30 minutes and the filtrate was identified using AAS.

3. **Result and Discussion**

3.1. Adsorbent Characterization

3.1.1. Scanning electron microscopy (SEM) and energy dispersive analysis (EDX). Morphological comparison between ACA and ACA-Fe_3O_4 is known through SEM analysis. In Figure 1, ACA has a morphology with highly visible pores (Fig. 1a) and ACA-Fe_3O_4 has a rough morphology (Fig. 1b). That has occurred because magnetite (Fe_3O_4) particles have coated the ACA surface. Figure 1c is the morphology of the ACA-Fe_3O_4 after Ni(II) adsorption test. Morphological of ACA-Fe_3O_4 surfaces has changed due to Ni(II) ions filled the pores which are supported with EDX data stated in Table 1.

3.1.2. X-ray powder diffraction. Phases of ACA and ACA-Fe_3O_4 were identified using XRD analysis with the peak X-ray diffraction standard for Fe_3O_4. The diffractogram of ACA (Figure 2a/ 2b) shows the wide peaks in the 2Θ region with degrees 23-30° and 40° indicating that the ACA phase is amorphous (a journal reference only). The Crystalline phase of magnetite (Fe_3O_4) and ACA-Fe_3O_4 particles was shown on a sharp diffractogram in the 2Θ region of each 30.21; 35.52; 43.07; and 57.16°.

Table 1. Elemental composition on ACA and ACA-Fe_3O_4

Sample	Elements (wt %)			
	C	O	Fe	Ni
ACA	80.74	19.26	-	-
ACA-Fe_3O_4	33.01	46.81	20.18	-
ACA-Fe_3O_4-Ni	43.75	50.64	5.50	0.11

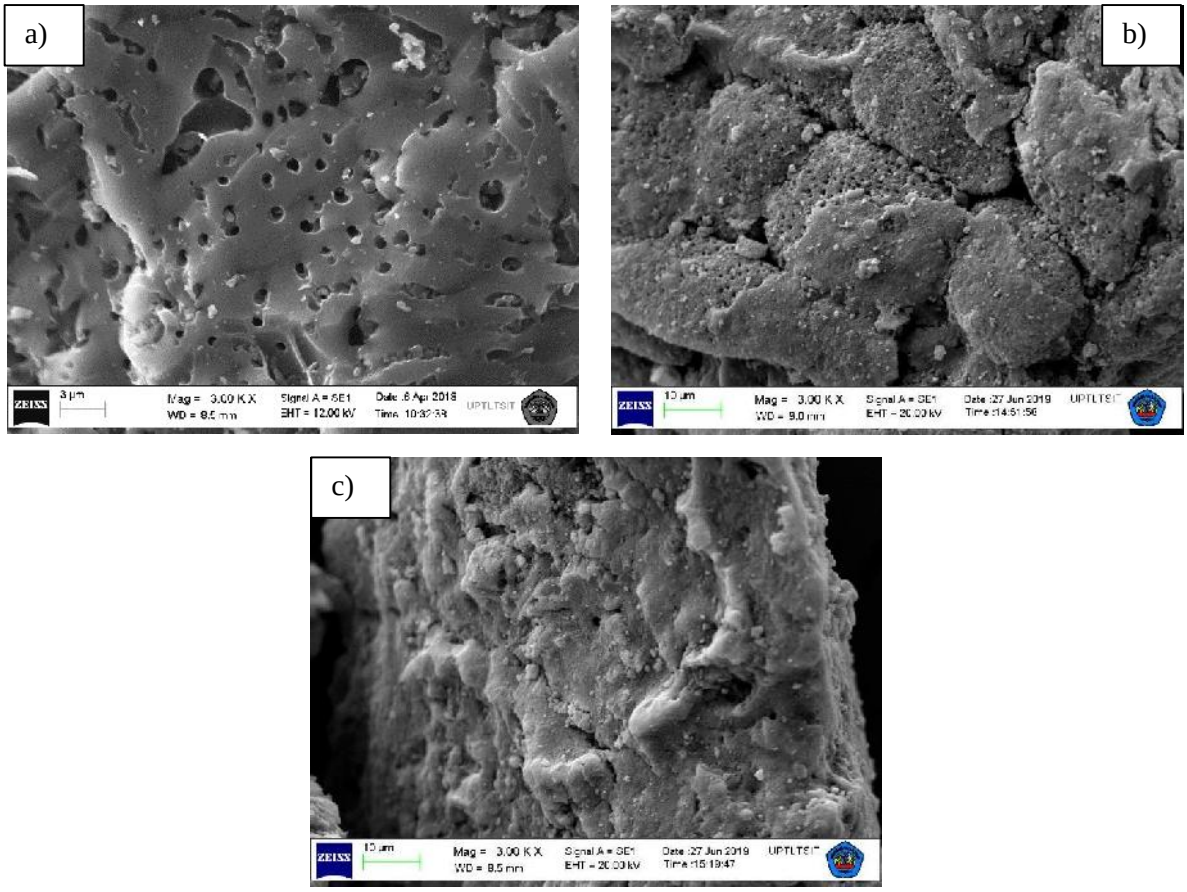

Figure 1. SEM images of a) ACA, b) ACA-Fe_3O_4, and c) ACA-Fe_3O_4 after adsorbing Ni(II) ions at 3000-time magnification

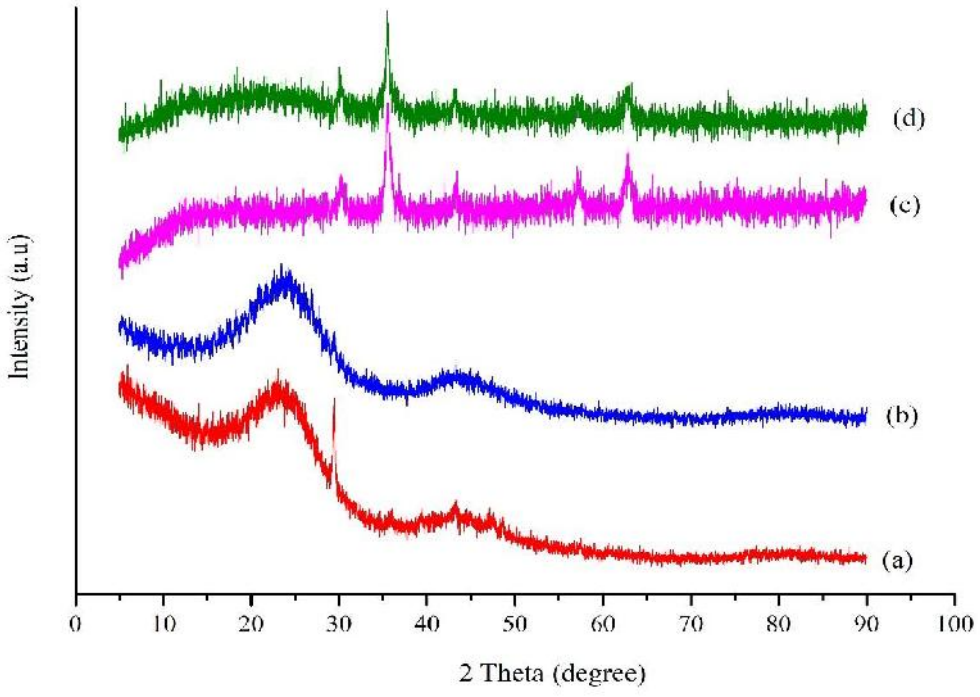

Figure 2. Diffractogram of a) AC b) ACA, c) magnetite, and d) ACA-Fe_3O_4

3.1.3. Surface area measurements. Surface area and pore volume in ACA and ACA-Fe_3O_4 are known from characterization using the BET surface area. The surface area and pore volume of the adsorbent are presented in Table 2. The results in Table 2 state that the high surface area of the adsorbent produces many active sites. The presence of magnetite particles (Fe_3O_4) lining the ACA surface causes a decrease in the surface area of ACA-Fe_3O_4. The surface area of ACA and ACA-Fe_3O_4 are 415.116 and 300.09 $m^2 \cdot g^{-1}$, respectively. Then the total pore volume value, BJH surface area, BJH pore volume, and pore average have increased in the presence of magnetite that coated the activated carbon.

Table 2. The results of the characterization using the BET (*surface area*) method on ACA and ACA-Fe_3O_4

Adsorbent Surface Characteristics	Adsorbent	
	ACA	ACA-Fe_3O_4
Total surface area ($m^2.g^{-1}$)	415.116	300.090
Total pore volume ($cm^3.g^{-1}$)	0.229	0.201
BJH surface area ($m^2.g^{-1}$)	17.136	20.089
BJH pore volume ($cm^3.g^{-1}$)	0.029	0.064
Average pore diameter (nm)	0.110	0.134

3.2. *Adsorption Test*

3.2.1. Effect of adsorbent dosage. The optimum dose was obtained at the use of 0.5 grams of adsorbent with an adsorption percentage of 99.11% (Figure 3). The more the dose was used, the more active sites of the adsorbent can adsorb Ni(II) ions.

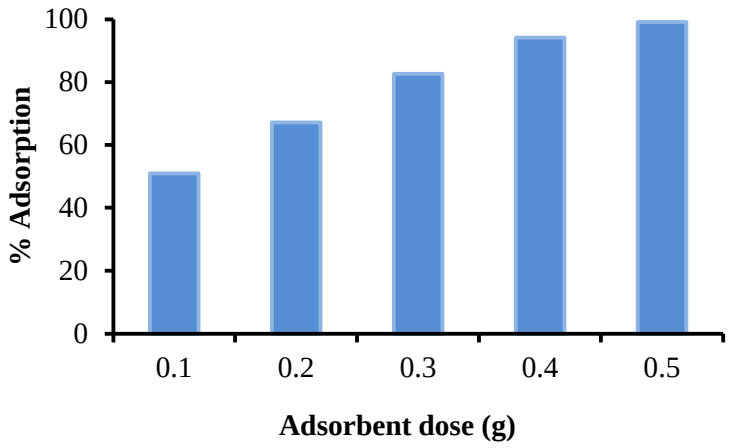

Figure 3. Effect of adsorbent dose on the adsorption percentage of Ni(II) ions in solution

3.2.2. Effect of pH. Variation of pH conducted in this study was to determine the effect of pH on the adsorption of Ni(II) ions in solution. Based on Figure 4, the change of pH has no significant effect on the adsorption of Ni(II) ions. Changes in pH to bases cause the deposition of Ni(II) ions at the beginning of the adsorption process.

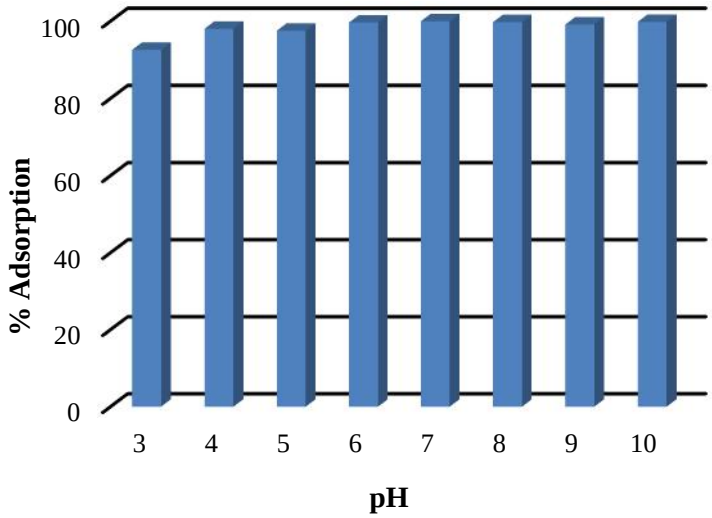

Figure 4. Effect of pH on the adsorption percentage of Ni(II) ions in solution

3.2.3. Effect of contact time. In this study to see the optimum contact time between adsorbents and adsorbate molecules was done by interacting 0.4 grams of adsorbent with 25 mL of 100 ppm Ni(II) ion solution with contact time variations of 15-90 minutes. Figure 5 states that the length of contact time affects the adsorption process. The longer contact time is used, the greater the adsorption rate. The optimum contact time was obtained at 90 minutes with adsorption of 32.122 and 65.815% for ACA and ACA-Fe_3O_4 respectively.

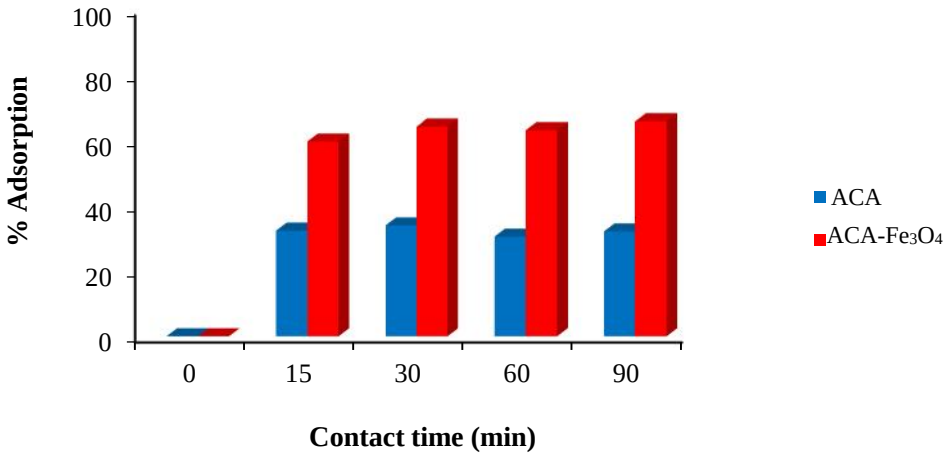

Figure 5. Effect of contact time on the adsorption percentage of Ni(II) ions in solution

The kinetics of Ni(II) ion adsorption were analyzed using pseudo-first-order (1) and pseudo-second-order (2) equations.

$$\ln(q_e - q_t) = \ln q_e - k_1 t \quad (1)$$

$$\frac{t}{q_t} = \frac{1}{k_2 q_e^{\,2}} + \frac{t}{q_e} \quad (2)$$

Information on the formula presented is qt is the number of ions adsorbed at different times ($mg \cdot g^{-1}$), qe is the number of ions adsorbed at equilibrium time ($mg \cdot g^{-1}$), t is time/minute, while k_2 shows the pseudo-second-order rate constant ($g \cdot mmol^{-1} \cdot min^{-1}$). Based on Figure 6, the adsorption of Ni(II) ions on ACA-Fe_3O_4 tends to follow the pseudo-second-order adsorption kinetics, indicated by a value of R^2 close to 1 (Table 3).

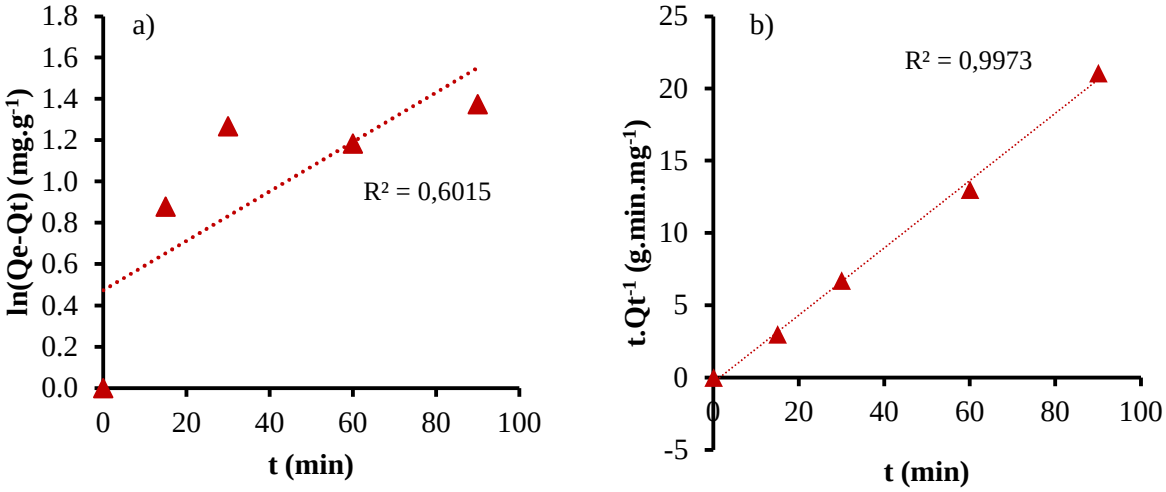

Figure 6. Graph of pseudo a) first-order and b) second-order for adsorption Ni(II) on ACA-$Fe_3O_4Fe_3O_4$

Table 3. Pseudo-first-order and second-order rate constant of ACA and ACA-Fe_3O_4

	Pseudo first order		Pseudo second order	
	k_1 (min^{-1})	R^2	k_2 ($g.mmol^{-1}.menit^{-1}$)	R^2
ACA	-	-	37,368	0,999
ACA-Fe_3O_4	0,012	0,602	9,543	0,997

3.2.4. Effect of concentration. The effect of the concentration of the adsorbate solution on the adsorption process can be determined by analysis using an adsorption isotherm model consisting of two types, namely Langmuir and Freundlich adsorption isotherms. The Langmuir and Freundlich adsorption isotherm model can be expressed in equations (3) and (4):

$$\frac{C}{m} = \frac{1}{bK} + \frac{C}{b} \quad (3)$$

$$\log q_e = \log k_f + 1/n \log C_e \quad (4)$$

In equation 3, C is the equilibrium concentration ($mg \cdot L^{-1}$), m is the amount of adsorbed substance per gram of adsorbent at concentration C ($mmol \cdot g^{-1}$), b represents the amount of adsorbed substance when saturated (adsorption capacity) ($mg \cdot g^{-1}$), and the adsorption equilibrium constant and the Freundlich capacity factor is expressed respectively with K ($L \cdot mol^{-1}$) and k_f ($(mg \cdot g^{-1})$ $(L \cdot mg^{-1})^{1/n}$). Whereas, qe is

the amount of substance adsorbed per gram of adsorbent (mmol·g^{-1}), Ce: concentration equal to adsorbate in the solution phase (mg·L^{-1}).

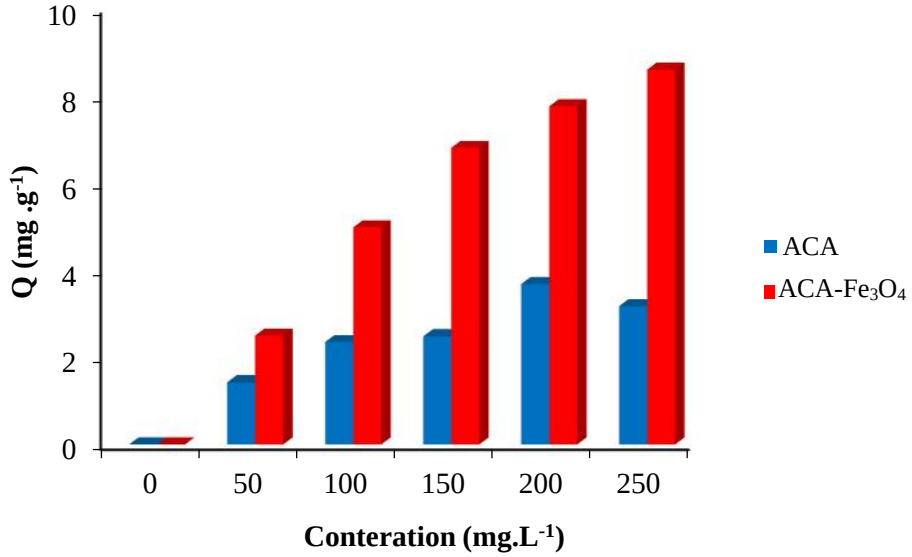

Figure 7. Influence of concentration on the sorption of Ni(II) cations in solution

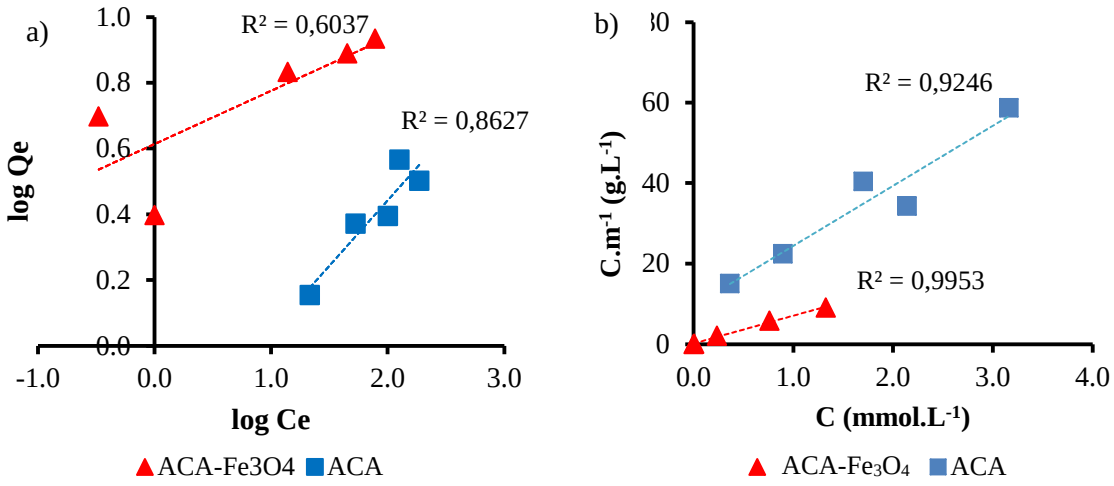

Figure 8. a) Freundlich and b) Langmuir adsorption isotherms of Ni(II) cations by ACA and ACA-Fe_3O_4

Based on Figure 7, an increase in the initial concentration of Ni(II) ions is accompanied by an increase in Q value which means that more Ni(II) ions are adsorbed by the adsorbent. The analysis in Figure 8 shows that the adsorption of Ni(II) ions on ACA and ACA-Fe_3O_4 follows the Langmuir adsorption isotherm model (Table 4). The adsorption process that occurs is dominated by chemical interactions between metal ions as adsorbates and the active site of the adsorbent [3].

Table 4. Isotherm parameters of Ni(II) ions sorption in solution by ACA and ACA-Fe_3O_4

Model		Adsorbent	
		ACA	ACA-Fe_3O_4
Langmuir			
	q_m in mg g^{-1}	3.933	8.495
	K_L in L mol^{-1}	1564.5	37650
	R^2	0.925	0.995
Freundlich			
	K_f in (mg g^{-1})(L mg^{-1})$^{1/n}$	2.251	0.243
	n	2.514	6.177
	R^2	0.863	0.604

3.3. Desorption Test

Desorption with a water solvent was expected to physically release Ni(II) ions from the adsorbent. Furthermore, the ethanol solvent contained hydroxyl OH^- group functions to release the adsorbate which is bound by hydrogen bonds. Then desorption was continued on the acid solvent, HCl to release the adsorbed chemically adsorbed through the interaction of ionic bonds [16]. EDTA solvents were used if the adsorbate is bound to form a complex compound. The results of desorption using HCl eluents in this study produced the best desorption rates for Ni(II) ions in ACA and ACA-Fe_3O_4 which was 24.42 and 70.84% respectively (Figure 9).

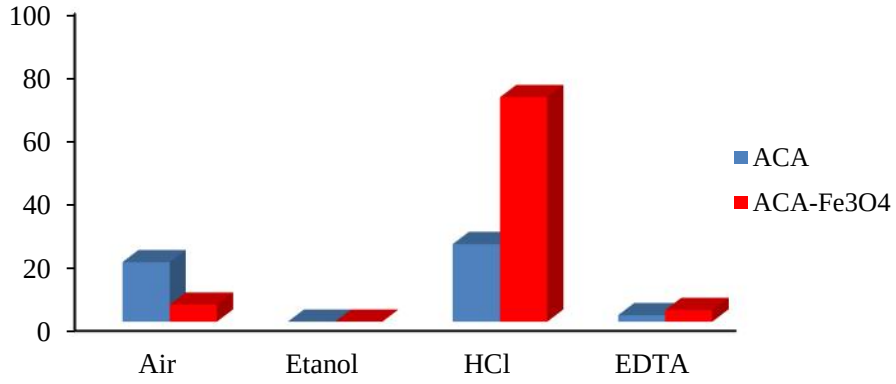

Figure 9. Desorption of Ni(II) ions with several types of eluents

4. Conclusion

Activated carbon obtained from palm shells coated with magnetite (ACA-Fe_3O_4) was a very effective adsorbent in the treatment of wastes containing Ni(II) ions in water resources. The optimum conditions of adsorption of Ni (II) with ACA-Fe_3O_4 were with 500 mg of adsorbent at 25 mL of 100 ppm adsorbate and a contact time of 1 hour with an adsorption percentage of 99.11%. The adsorption of Ni(II) ions on ACA-Fe_3O_4 tends to follow the pseudo-second-order kinetics and the Langmuir adsorption isotherm model. Desorption process with HCl as eluent was produced the best desorption rate of 70.84%.

Acknowledgments

We be grateful to the Directorate of Research and Community Service, Directorate-General for Research and Development, Ministry of Research, Technology and Higher Education of the Republic of Indonesia for funding this work with the number of contract: 179/SP2H/AMD/LT/DRPM/2020. We also give thanks to the Technical Service Unit of the Integrated Laboratory and the Technology Innovation

Center–University of Lampung (UPT Laboratorium Terpadu dan Sentra Inovasi Teknologi–Universitas Lampung) for its hospitality.

References

[1] Kausar R, Buhani, and Suharso 2020 Methylene blue adsorption isotherm on *spirulina* sp. microalgae biomass coated by silica-magnetite *Mater. Sci. Eng.* **857** 1-7
[2] Khuluk R H, Rahmat A, Buhani, and Suharso 2019 Removal of methylene blue by adsorption onto activated carbon from coconut shell (cocous nucifera l) *Indones. j. sci. technol.* **2** 229-240
[3] Buhani B, Herasari D, Suharso S, and Yuwono S D 2017a Correlation of ionic imprinting cavity sites on the amino-silica hybrid adsorbent with adsorption rate and capacity of cd^{2+} ion in solution. *Orient. J. Chem.* **33** 418-429
[4] Permatasari D, Buhani, Rilyanti M, and Suharso 2020 Adsorption isotherm of multicomponent solution of Cu(II) ions, crystal violet, and methylene blue on silica-magnetite porphyridium sp. algae hybrid *Mater. Sci. Eng.* **857** 1-8
[5] Suharso, Buhani, and Sumadi 2010 Immobilization of s. duplicatum supported silica gel matrix and its application on adsorption-desorption of Cu(II), Cd(II), and Pb(II) ions *Desalination* **263** 64-69
[6] Chen Y, Zhao W, Zhao H, Dang J, Jin R, and Chen Q 2020 Efficient removal of Pb(II), Cd(II), Cu(II) and Ni(II) from aqueous solutions by tetrazole-bonded bagasse *Chemical Physics* **529** 1-7
[7] Buhani, Suharso, and Satria H 2011 Hybridization of nannochloropsis sp biomass-silica through sol-gel process to adsorb Cd(II) ion in aqueous solutions *Eur J. Sci. Res.* **51** 467-476
[8] Raval N P, Prapti U, Shah, Nisha K, and Shah 2016 Adsorptive removal of nickel(II) ions from aqueous environment: a review *J. Environ. Manage.* **179** 1-20
[9] Runtti H, Tuomikoski S, Kangas T, Lassi U, Kuokkanen T, and Ramo J 2014 Chemically activated carbon residue from biomass gasification as adsorbent for iron(II), copper(II) and nickel(II) ions. *J. Water Process Eng.* **4** 12-24.
[10] Kaur N, Kaur M, and Singh D 2019 Fabrication of mesoporous nanocomposite of graphene oxide with magnesium ferrite for efficient sequestration of Ni(II) and Pb(II) ions adsorption, thermodynamic and kinetic studies *Environ. Pollut.* **253** 111-119
[11] Buhani, Suharso, Aditiya I, Kausar R A, Sumadi, and Rinawati 2019a Production of a spirulina sp. algae hybrid with a silica matrix as an effective adsorbent to absorb crystal violet and methylene blue in a solution *Sustain. Environ. Res.* **29** 1-11
[12] Issabayeva G, Aroua M K, and Sulaiman N M 2010 Study on palm shell activated carbon adsorption capacity to remove copper ions from aqueous solutions *Desalination* **262** 94-98
[13] Wang S and Li F 2013 Invertase SUC2 is the key hydrolase for inulin degradation in saccharomyces cerevisiae *J. Appl. Environ. Microbiol.* **79** 403-406
[14] Buhani, Puspitarini M, Rahmawaty, Suharso, Rilyanti M, and Sumadi 2018a Adsorption of phenol and methylene blue in solution by oil palm shell activated carbon prepared by chemical activation *Orient. J. Chem.* **34** 2043-2050
[15] Buhani, Suharso, and Sumadi 2010 Adsorption kinetics and isotherm of Cd(II) ion on nannochloropsis sp biomass imprinted ionic polymer *Desalination* **259** 140-146
[16] Buhani, Suharso, Rilyanti M, and Sumadi 2018b Implementation of sequential desorpsion in determining Cd(II) ion interaction with adsorbent of ionic imprinting amino-silica hybrid *Rasayan J. Chem.* **11** 865-870
[17] Anshar A M, Taba P, and Raya I 2016 Kinetic and thermodynamics studies the adsorption of phenol on activated carbon from rice husk activated by $ZnCl_2$ *Indones. J. Sci. Technol.* **1** 47-60
[18] Buhani, Hariyanti F, Suharso, Rinawati, and Sumadi 2019b Magnetized algae-silica hybrid from porphyridium sp. biomass with Fe_3O_4 particle and its application as adsorbent for the removal of methylene blue from aqueous solution. *Desalin. Water Treat.* **142** 331-340

[19] Buhani, Suharso, Luziana F, Rilyanti M, and Sumadi 2019c Production of Adsorbent from Activated Carbon of Palm Oil Shells Coated by Fe_3O_4 Particle to Remove Crystal Violet in Water. *Desalin. Water Treat.* **171** 281-293
[20] Buhani, Musrifatun, Pratama D S, Suharso, and Rinawati 2017b Modification of chaetoceros sp. biomass with silica-magnetite coating and adsorption studies towards Cu(II) ions in single and binary system. *Asian J. Chem.* **29** 2734-2738
[21] Nejadshafiee V and Islami M R 2019 Adsorption capacity of heavy metal ions using sultone-modified magnetic activated carbon as a bio-adsorbent *Mater. Sci. Eng.* **101** 42–52
[22] Nandiyanto A B, Putra Z A, Andika R, Bilad M R, Kurniawan T, Zulhijah R, and Hamidah I 2017 Porous activated carbon particles from rice straw waste and their adsorption properties. *J. Eng. Sci. Technol.* **12** 1-11
[23] Nandiyanto A B D, Zaen R, and Oktiani R 2018 Working Volume in High-Energy Ball-Milling Process on Breakage Characteristics and Adsorption Performance of Rice Straw Ash *Arab. J. Sci. Eng)* **43**(11) 6057-6066
[24] Pamidimukkala P S and Soni H 2018 Efficient removal of organic pollutants with activated carbon derived from palm shell: spectroscopic characterisation and experimental optimization. *J. Environ. Chem. Eng.* **6** 3135-3149
[25] Ebadollahzadeh H and Zabihi M 2020 Competitive adsorption of methylene blue and Pb (II) ions on the nano-magnetic activated carbon and alumina *Mater. Chem. and Phys.* **248** 1-16
[26] Buhani, Suharso, and Aprilia L 2012 Chemical stability and adsorption selectivity on cd^{2+} ionic imprinted *nannochloropsis sp* material with silica matrix from tetraethyl orthosilicate. *Indo. J. Chem.* **12** 94-99
[27] Buhani, Narsito, Nuryono, Kunarti E S, and Suharso 2014 Adsorption competition of Cu(II) ion in ionic pair and multi-metal solution by ionic imprinted amino-silica hybrid adsorbent. *Desalin. Water Treat.* 1-13
[28] Mohan D, Sarswat A, Singh V K, Franco M A, Charles U, and Pittman Jr 2011 Development Development of Magnetic Activated Carbon from Almond Shells for Trinitrophenol Removal from Water. *Chem. Eng. J.* **172** 1111-1125